◆◆◆ Scientific
◆◆◆ Research

Carbonation Resistance and Anticorrosive Properties of Organic Coatings for Concrete Structures

Theodosia Zafeiropoulou, Eleni Rakanta, George Batis

Department of Materials Science and Engineering, School of Chemical Engineering, National Technical University of Athens, Athens, Greece.
Email: dia_zaf@mail.ntua.gr, erakanta@central.ntua.gr, gbatis@central.ntua.gr

ABSTRACT

The present study examines the behavior of three major categories of organic coatings which are applied on the surface of concrete structures and specifically conventional, high performance and nanotechnology paint systems. The comparison is achieved in the means of anticorrosion properties under the presence of chloride ions and carbonation resistance. The evaluation methods included electrochemical measurements in order to assess corrosion properties and the determination of steel's mass loss after the end of the experimental procedure. Carbonation depth was measured using phenolphthalein as indicator after accelerated and physical exposure. From the results so far it can be shown nanocoatings gave promising results regarding induced chloride ion corrosion.

Keywords: Chloride Induced Corrosion; Electrochemical Measurements; Carbonation; Concrete

1. Introduction

Corrosion of steel reinforcement is one of the most significant factors in the deterioration of reinforced concrete structures especially those located near to marine and industrial areas. Rebars' corrosion, carbonation of concrete and chloride attack affects almost 50% the durability of concrete structures [1]. Earlier studies indicated that reinforced concrete structures remain durable for the whole of their design life, approximately more than 60 years [2-4], even maintenance-free. However, the corrosion of rebars affects the life of the concrete and thus has rapidly become a serious problem throughout the world. Parking structures, bridges, buildings, and other reinforced concrete structures exposed to aggressive environments are being severely damaged due to corrosion of reinforcing steel within periods as short as 10 - 20 years [5]. The two most common mechanisms of reinforcement corrosion are: 1) *Localized destruction of the passive film when diffused chloride ions reach the rebar's surface through porous concrete*. The steel rebar inside reinforce concrete structures is susceptible to corrosion when permeation of chloride from deicing salts or seawater results in the chloride content at the surface of the steel exceeding a chloride threshold level which can be defined as the content of chloride at the steel depth that is necessary to sustain local passive film breakdown and hence initiate the corrosion process [6]. 2) *Carbonation*. Atmospheric CO_2 reacts with $Ca(OH)_2$ under the presence of water

and as a result the alkalinity value of concrete reduces down to 9. This pH value is leading to a general breakdown in passivity and as a result rebars are starting to corrode [7]. Organic coatings are widely used in concrete structures for decorative, as well as protection purposes, since they consist of a barrier between the porous concrete structure and the corrosive environment. Usually, conventional coatings based on acrylic emulsions are used for indoor and outdoor applications and exhibit a satisfying protection level. High-performance anticorrosion coatings are applied to concrete structures to provide protection from corrosive industrial environments. Generally, they are separated into two major categories: 1) Protective coatings applied to structures in oil, gas, petrochemical and power generation industries, as well as to bridges and water and waste treatment plants. 2) Marine coatings applied to commercial ships, including freight carriers, tows, cruise ships and others. Nanotechnology coatings have recently been introduced and have been in wide use since then due to their significant properties which include high radiation resistance, antibacterial properties and high breathability. In order to be considered as efficient an organic coating is demanded to have numerous of properties, including low penetration values and high mechanical resistance [8]. From the category of traditional paints, it has been found that elastomeric coatings can provide a satisfying protection level against chloride corrosion and they also exhibit good physicochemical properties. Acrylic paints demonstrated promis-

ing results regarding induced corrosion and carbonation [9]. It has also been reported that polyurethane coatings are offering high resistance to the corrosion process and chlorinated rubber coatings demonstrate an increasing tendency regarding polarization resistance values. Epoxy coatings are also sufficient in rebar's protection [10]. Nanotechnology paints appeared more effective compared to traditional coatings for a short period of time regarding anticorrosive behavior and exhibited improved physicochemical properties. In the means of adhesion resistance it can was shown that nano-coatings were more durable than traditional acrylic and elastomeric dispersions [11]. However, long term corrosion inspection has not been investigated for novel coating systems as well as anticarbonation performance and this consists of the objective of the present study.

2. Materials

2.1. Cement Mortar Specimens

Reinforced and plain cement mortar specimens were constructed in the present study. The test specimens were prepared with cement, sand and water in ratio 1:3:0.5. The mean value of the Greek quarry sand diameter was 250 μm < d < 4 mm, the cement type used was Cement II 32.5 N and the water was drinkable from NTUA water supply, appropriate for preparing specimens according to ELOT 452 [12]. Cylindrical steel rebars of type B500C with dimensions of 12 mm in diameter and 10 mm high were used for the reinforced test specimens. The rebars meet Greek specifications of Hellenic Organization for Standardization, ELOT 1421-3 [13]. Fabrication of the steel for the test specimens simply involved cutting to the consistent length of 100 mm. The test specimens considered for the present study were cylindrical 100 mm in height and 40 mm in diameter. Each contained one steel rebar in the position shown in **Figure 1**. The cement mortar constituents were mixed in a mortar mixer for approximately 5 minutes, till a uniform consistency was achieved. The molds (100 mm in height and 40 mm in diameter) were filled with mortar and vibrated for consolidation using a vibrating table. Copper wire cables were connected to the steel bar for electrochemical measurements. Prior to the preparation, the steel surface was cleaned according to the ISO/DIS 8407.3 Standard [14]. In particular the surface of the steel bars was washed with water and then immersed in strong solution of HCl with organic corrosion inhibitor for 15 min, washed with water and washed thoroughly with distilled water to eliminate traces of the corrosion inhibitor and chloride ions. Following that, the surface was cleaned with alcohol and acetone and finally weighed to accuracy of 0.1 mg. Thereafter, the bars were placed in cylindrical molds, as shown in **Figure 1**.

The mortars were cast and stored at ambient condi-
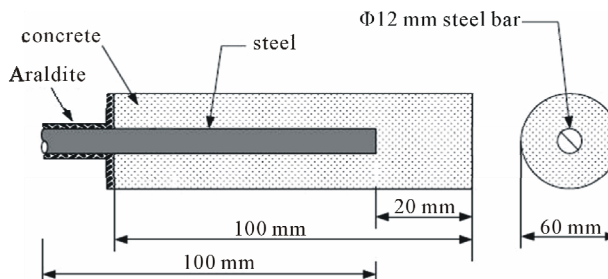
Figure 1. Schematic representation of reinforced mortar specimen.

tions in the laboratory for 24 hours. After being demolded, the specimens were placed in water in curing room (RH > 98%, T = 20°C ± 1.5°C) for 24 hours and then kept for an additional 7 days at ambient temperature, in a laboratory environment to stabilize internal humidity, followed by insulation with epoxy resin of the region shown in **Figure 1**. Finally the specimens were partially immersed in 3.5% wt NaCl solution, up to 20 mm from the bottom. The objective of partially immersing the cement mortar specimens was to provide an increase of required moisture and oxygen for the initiation and acceleration of reinforcement corrosion. The chloride concentration of the exposure solution was selected in order to stimulate marine environment. The experimental duration of this study was 15 months.

2.2. Organic Coatings

Organic coatings were applied by brush on the dried surface of the specimens at two layers, the second layer 24h after the first one. The composition of the coatings used is given in **Table 1**. Dry film thickness of all coatings was measured using ultrasonic thickness gauge meter according to ASTM D 6132-08 [14] Standard Test Method [15]. Three different organic coatings were tested from each major category. For conventional coatings an acrylic paint, an elastomeric-acrylic resin dispersion and a silicon-acrylic paint were used. Apart from the resin, there are differences in other technical characteristics such as in density or viscosity of every coating. Regarding high performance coatings in the present study an epoxy, a polyurethane and a chlorinated rubber coating were evaluated, which exhibit different characteristics and they are also applied in variant cases. Finally, for nanotechnology paint systems a siloxane coating, a pure acrylic paint and an elastomeric-nano acrylic coating were contrasted with various dilution percentages and characteristics.

3. Evaluation Methods

After the construction and the application of the coatings, specimens were exposed to corrosive environments in

Table 1. Chemical composition of organic coatings.

Nomeclature/Thickness (μm)	Description
Ref	Specimens without coating application
Conv_1/250	Acrylic paint for exterior use, acrylic resin dispersion, solids b.w.: 61% ± 2.5%. Diluted 10% v/v with water. Density: 1.46 ± 0.05 g/ml, viscosity: 107 ± 13 KU, spreading rate: 9 m²/l
Conv_2/250	Solvent based primer for exterior use (solids b.w.: 26% ± 2%) dilution 100% white spirit. Elastomeric, insulating paint for horizontal surfaces, acrylic resin dispersion, solids b.w.: 62% ± 1%. No dilution. Density: 1.37 ± 0.05 g/ml, viscosity: 107 ± 13 KU, spreading rate: 1.5 m²/l
Conv_3/250	Silicon acrylic water-repellent paint, for exterior use, silicon acrylic resins, solids b.w.: 64% ± 1.5%. Diluted 10% v/v with water. Density: 1.52 ± 0.04 g/ml, viscosity: 100 ± 6 KU, spreading rate: 8 ± 0.5 m²/l
HP_1/300	Two-component, anticorrosive epoxy primer (solids 58%). Two component pure epoxy paint, hardened with amine. Solids b.w.: 95%. Spreading rate: 6m²/kg
HP_2/400	Two-component, anticorrosive epoxy primer (solids 58%). Two component pure epoxy paint, hardened with amine. Solids b.w.: 95%. Two-component polyurethane paint with aliphatic isocyanate. Solids b.v.: 54%. Spreading rate: 9 - 11 m²/l
HP_3/250	Primer with special resins. Liquid rubber acrylic based sealant. Density: 1.37 ± 0.5 g/cm³
Nano_1/200	Water based siloxane self-clean coating, solids b.v.: 50%. Diluted 10% with water. Spreading rate: 6 - 8 m²/l
Nano_2/200	Nanotechnology paint system, 100% acrylic resin, solids b.v.: 64%. Diluted 5% v/v with water. Spreading rate: 6 - 9 m²/l
Nano_3/200	Primer with siloxanes in organic solvent. Elastomeric nano-acrylic emulsion, solids b.v.: 50% ± 3%. No dilution. Viscosity: 125 ± 5 KU, spreading rate: 5 m²/l

order to evaluate their protection level against induced chloride corrosion and carbonation. Six reinforced specimens from each coating were partially immersed in 3.5 wt% NaCl solution for 15 months and during this period electrochemical measurements were conducted including half-cell potential and linear polarization technique. After the end of the exposure period the mass loss of the embedded rebars was determined. Six plain cement mortar specimens covered with each coating were exposed to both physical and high concentration CO_2 environment, in order to determine carbonation depth.

3.1. Corrosion Evaluation

3.1.1. Half-Cell Potential Measurements (HCP)

For a period of 15 months steels' half-cell potential was periodically measured versus a SCE, according to ASTM C876-87 [16]. Half-cell potential measurements of steel rebars is the most typical procedure to the routine inspection of reinforced concrete structures regarding the corrosion trend of the samples. Potential readings are highly influenced by the surface treatment of the specimens which causes changes in their resistivity, as long as the constituents of the cement mortars remain the same However, they are not sufficient as criterion since they are affected by number of factors, which include polarization by limited diffusion of oxygen, concrete porosity and the presence of highly resistive layer [17].

3.1.2. Linear Polarization Technique (LPR)

Tests were conducted using a Potentiostat/Galvanostat Model 263A from EG&G Princeton Applied Research and an associated software package to analyze the obtained data. The electrochemical parameter of polarization resistance (R_p) was defined as described in ASTM G59-97(2009) [18]. The experimental set up was consisted of three electrodes where steel rebars represented the working electrode, saturated calomel electrode (SCE) the reference electrode and a carbon bar served as the counter electrode. The potential scan range was ± 10 mV from Open Circuit Potential (OCP) and the scan rate was 0.166 mV/s. Linear Polarization technique is a corrosion monitoring method that allows corrosion rates to be measured directly, in real time. The technique is rapid and non-intrusive, requiring only a connection to the reinforcing steel. In LPR measurements the reinforcing steel is perturbed by a small amount from its equilibrium potential. This can be accomplished potentiostatically by changing the potential of the reinforcing steel by a fixed amount, ΔE, and monitoring the current decay, ΔI, after a fixed time. The polarization resistance, R_p, of the steel is then calculated from Equation (1),

$$R_p = \frac{\Delta E}{\Delta I} \tag{1}$$

From which the corrosion rate, I_{corr}, can then be calculated

$$I_{\text{corr}} = \frac{\beta_a \cdot \beta_c}{2.303 \cdot (\beta_a + \beta_c)} \cdot \frac{1}{R_p} = \frac{B}{R_p} \tag{2}$$

where β_a, β_c are the anodic and cathodic Tafel slopes respectively and R_p is the polarization resistance (Ohm). For Stern-Geary constant B a value of 26 mV has been adopted for active corroding steel bars and 52 mV for passive conditions. In order to determine the corrosion current density, i_{corr}, the surface area, A, of steel that has been polarized needs to be accurately known:

$$i_{corr} = \frac{I_{corr}}{A} \qquad (3)$$

Obtained R_p values are highly correlated with a number of factors, including surface treatment, corrosive environment and the materials that were used for the construction of the specimens. In the present study the corrosive environment as well as the materials of the specimens remained stable and consequently all changes to R_p values are due to differences in the surfaces treatment.

Define abbreviations and acronyms the first time they are used in the text, even after they have been defined in the abstract. Abbreviations such as IEEE, SI, MKS, CGS, sc, dc, and rms do not have to be defined. Do not use abbreviations in the title or heads unless they are unavoidable.

3.2. Mass Loss Determination

To evaluate corrosion from chloride ions 6 mortar specimen for every coating were broken open and the final weight of the steels after de-rusting and cleaning was obtained. The average mass loss was calculated from the difference between the initial and the final mass of each steel bar.

3.3. Carbonation Resistance

Carbonation damage usually occurs when there is little concrete cover over the reinforcing steel and proceeds mainly by diffusion. However, it is possible for a concrete to carbonate even when the cover depth to the reinforcing steel is high and this may be due to a very open pore structure where pores are well connected together and allow rapid CO_2 ingress. Generally, carbonation threshold for the initiation of reinforcement corrosion is when carbonation depth exceeds the concrete or cement mortar cover [19].

3.3.1. Accelerated Carbonation Chamber

After 3 weeks in an accelerated carbonation chamber in an environment of 10% v/v CO_2, the specimens were split into two halves and a phenolphthalein indicator (1% phenolphthalein solution in ethanol) was sprayed onto their cut surfaces in order to visualize the carbonation front according to RILEM CPC-18 [20]. Purple colored areas indicate uncarbonated mortar specimen whereas carbonated areas remain colorless.

The carbonation depth that was measured after the exposure of the specimens to an accelerated carbonation chamber was used to calculate the carbonation coefficient K according to Equation (4) as follows [21]:

$$x = K\sqrt{t} \qquad (4)$$

where K is the carbonation constant (cm/s 0.5), x is the carbonation depth (cm) and t is the time (s).

If uncoated and coated cement mortar surfaces are exposed to CO_2 environment for the same period of time, then:

$$t_0 = t \Rightarrow \frac{1}{K^2} x_0^2 = \frac{1}{K^2} x^2 + \frac{1}{K^2} \frac{2D}{d} x \qquad (5)$$

where t_0, t are the periods of time (s) for uncoated and coated cement mortar specimens, respectively and x_0, x are the carbonation depths (cm) for uncoated and coated cement mortar specimens, respectively, D is the diffusion coefficient (m^2/s) which in carbonated cement mortars equals to 2.4×10^{-8} m^2/s [22] and d is the total diffusion coefficient of the coating (m/s). Equation (5) is leading to:

$$d = \frac{2 \cdot D \cdot x}{x_0^2 - x^2} \qquad (6)$$

It is usual to compare the resistance of the coating with the resistance of another layer, composed of an imaginary air layer. The diffusion equivalent air layer thickness S_d (m) can be calculated from:

$$S_d = \frac{D_{air}}{d} \qquad (7)$$

where D_{air} is the free-air diffusion coefficient which equals to 153×10^{-7} m^2/s [21]. Diffusion resistance number μ (unitless) for each coating can be calculated from:

$$\mu = \frac{S_d}{S} \qquad (8)$$

where S is the thickness of the coating (m).

3.3.2. Physical Exposure

Plain cement mortar specimens were exposed to physical conditions in laboratory environment for a period of 15 months and the carbonation depth was measured following the same procedure as before.

4. Results and Discussion

4.1. Corrosion Evaluation

4.1.1. Half-Cell Potential Measurements (HCP)

In **Figure 2(a)**, are presented the corrosion potentials as a function of exposure time for cement mortars specimens covered with organic coatings and immersed in 3.5 wt% NaCl solution for a period of 15 months. The figure depicts the best coatings from every category and uncoated specimens for comparison reasons.

The interpretation of the results is achieved according to **Table 2** [19]. As it is shown at the end of the exposure period all specimens presented corrosion potential values that are indicative of severe corrosion and only HP_2 coating attained values that revealed intermediate to high

(a)

(b)
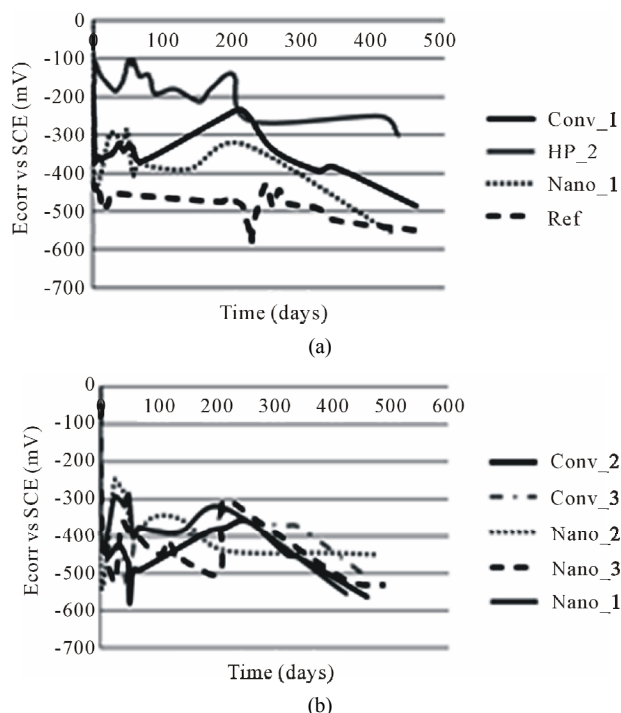
Figure 2. (a) Average half-cell potential values for six specimens as a function of exposure time for reinforced cement mortars partially immersed in 3.5 wt% NaCl solution; (b) Comparison between conventional and nanotechnology based coatings regarding corrosion potential after 15 months of immersion in 3.5 wt% NaCl solution.

Table 2. Corrosion potential and corrosion condition.

Steel's corrosion potential vs SCE (mV)	Corrosion condition
>−126	Low (10% risk of corrosion)
−126 to −276	Intermediate corrosion risk
<−276	High (90% risk of corrosion)
<−426	Severe corrosion

risk of corrosion. The best nano-coating attained lower corrosion potentials than the traditional coating with the best behavior, but as it is shown to **Figure 2(b)** nano-coatings presented similar behavior with the other two conventional paint systems.

For all specimens Ecorr reduction to such electronegative values versus time is due to chloride induced corrosion and indicates that all steel rebars are in an active corrosion state, regardless the applied coating on cement mortars' surface. Such electronegative values are not surprising because they are in agreement with what reported by other authors [23,24]. However, corrosion potential measurements can be misleading because they measure the corrosion condition and not the corrosion rate and consequently they do not provide information regarding the thermodynamics of the corrosion.

4.1.2. Linear Polarization Technique (LPR)
Linear polarization measurements were periodically performed to six specimens for each coating and polarization resistance (Rp) values are presented in **Table 3**. The given values correspond to the specimens covered with the coatings that performed best from each category.

According to **Table 4** [19], after one year of exposure to the corrosive environment only specimens covered with HP_2 coating remain in passive condition. Regarding nano-coatings, it should be noted that Nano_1 demonstrated better behavior compared to all conventional coatings.

4.2. Mass Loss Results

The results of the weight loss of steel rebars after 15 months of partially immersion in 3.5 wt% NaCl solution are given in **Figure 3**. For every coating 6 specimens were used in order to obtain the following results.

The rebars of the cement mortar specimens that were covered with high performance coatings indicated the lowest mass loss values, which is in accordance with the electrochemical results. Regarding nano-coatings, Nano_1 coating demonstrated improved behavior since it presented lower values than all conventional coatings.

4.3. Carbonation Resistance Results

4.3.1. Accelerated Carbonation Chamber
Cement mortar specimens were exposed to an accelerated carbonation chamber in an environment of 10% v/v CO_2 for a period of 3 weeks. The estimation of the total diffusion coefficient d (m/s) of the coating was performed according to the Equation (6). In **Table 5** are presented the results for the specimens after the exposure in the carbonation chamber.

The coating with the best behavior towards induced chloride ion corrosion was chosen for accelerated carbonation. From the results it can be observed that the high performance coating presented no carbonation, whereas both conventional and nano-coatings exhibited
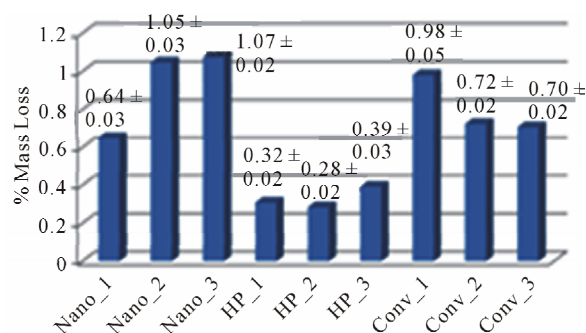
Figure 3. Average values of gravimetric mass loss and standard deviation after 15 months of immersion in 3.5 wt% NaCl solution.

Table 3. Average values of polarization resistance R_p and standard deviations.

Time (days)	R_p ($\Omega \cdot cm^2$)			
	Conv_3	HP_2	Nano_1	Reference
0	121,779 ± 294	331,240 ± 512	59,937 ± 114	0
13	-	427,939 ± 709	117,624 ± 122	
40	113,512 ± 174	498,795 ± 821	128,213 ± 156	22,509 ± 285
63	-	346,374 ± 483	126,609 ± 224	
70	-	267,742 ± 634	103,584 ± 324	
82	-	258,270 ± 456	-	
94	-	384,124 ± 657	-	
101	-	193,780 ± 533	175,651 ± 320	48,003 ± 331
125	148,819 ± 322	227,601 ± 240	-	33,032 ± 129
245	-	425,955 ± 612	177,030 ± 611	
269	-	254,592 ± 296	-	
455	161,987 ± 246	349,394 ± 509	90,116 ± 544	32,542 ± 312
479	-	454,840 ± 624	-	

Table 4. Polarization resistance values and corresponding corrosion rate [19].

R_p (k$\Omega \cdot cm^2$)	Corrosion rate
>260	Passive condition
52 - 260	Low to moderate corrosion
26 - 52	Moderate to high corrosion
<26	High corrosion rate

Table 5. Calculation of the equivalent air layer thickness, S_d.

Coating	x_0 (mm)	x (mm)	d (m/s)	D (m^2/s)	S (μm)	μ	S_d (m)
Nano_1	8	7.5	4.64×10^{-5}	2.4×10^{-8}	200	1646	0.33
HP_2	8	0	-	2.4×10^{-8}	400	-	-
Conv_1	8	4	4×10^{-6}	2.4×10^{-8}	250	15,300	3.83
Conv_3	8	7.5	4.65×10^{-5}	2.4×10^{-8}	250	1317	0.33

carbonated areas. However, it should be noted that carbonation depths varied in conventional systems where the acrylic-silicon dispersion presented almost double value than the acrylic coating.

4.3.2. Physical Exposure

After 15 months of physical exposure, cement mortar specimens were broken open and the carbonation depth was measure using phenolphthalein indicator. The results are presented in **Table 6**.

According to **Table 6** high performance coatings did not carbonate after 15 months of exposure whereas conventional coatings and Nano-coatings were carbonated 1 mm or 2 mm. in **Figure 4** are presented the measurements of the carbonation depth using phenolphthalein indicator which was sprayed in the left side of the mortars. Carbonated areas were revealed after the application of the indicator in nano and conventional coatings.
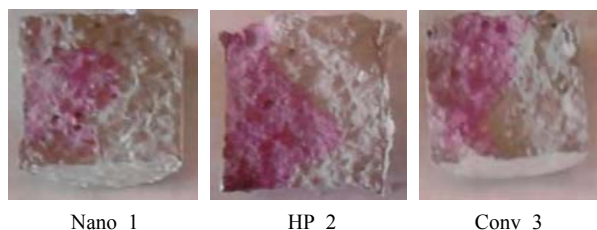
5. Conclusions

In the present study nine organic coating systems from

       JSEMAT

Table 6. Carbonation depth after one year of physical exposure.

	Nano			HP			Conv			Ref
	1	2	3	1	2	3	1	2	3	
Carbonation depth (mm)	2	1	1	0	0	0	1	1	2	3

Nano_1   HP_2   Conv_3

Figure 4. Carbonation depth after the application of the phenolphthalein indicator in the left side of the mortar.

three major categories were studied regarding their protection level against corrosion by chloride ions and carbonation, which are the two most common mechanisms of reinforcement corrosion. In marine areas there is a significant probability for rebars to be corroded by chloride ions, while carbonation problem exists in rural environment and in the interior of the structures. From the results, the following can be drawn:

- High performance coatings and specifically the polyurethane coating exhibited the most protective behavior against chloride induced corrosion as it presented the highest R_p values and very low mass loss values. Regarding carbonation, in both physical and accelerated exposure, no carbonated areas were revealed. However, it should be noted that high performance systems are environmentally harmful due to the organic solvents that contain.
- Regarding nano-coatings, Nano_1 coating appeared improved than conventional coatings towards chloride ions corrosion, whereas the other two nano-systems were equal with the traditional coatings. As far it concerns carbonation, Nano_1 coating appeared rather weak, since in both physical and accelerated conditions did carbonate more than Conv_1 coating. Its behavior, however, was not worse than the silicon-acrylic traditional system.

REFERENCES

[1] P. A. M. Basheer, S. E. Chidiac and A. E. "Long, Predictive Models for Deterioration of Concrete Structures," *Construction and Building Materials*, Vol. 10, No. I, 1996, pp. 27-37. doi:10.1016/0950-0618(95)00092-5

[2] F. E. Turnearsure and E. R. Maurer, "Principles of Reinforced Concrete Constructions," John Wiley & Sons, New York, 1955.

[3] Building Research Establishment, "Durability of Steel in concrete. Part I. Mechanism of Protection and Corrosion," Building Research Station, Watford, 1982, pp. 1-8.

[4] F. M. Lea, "Chemistry of Cement & Concrete," Edward Arnold Publishers Ltd., London, 1956.

[5] P. Venkatesan, N. Palaniswamy and K. Rajagopal, "Corrosion Performance of Coated Reinforcing Bars Embedded in Concrete and Exposed to Natural Marine Environment," *Progress in Organic Coatings*, Vol. 56, No. I, 2006, pp. 8-12. doi:10.1016/j.porgcoat.2006.01.011

[6] P. Schiessl and M. Raupach, "Influence of Concrete Composition and Microclimate on the Critical Chloride Content in Concrete," In: C. L. Page, K. W. J. Treadaway and P. B. Bamforth, Eds., *Corrosion of Reinforcement in Concrete*, Elsevier Applied Science, London, 1990, pp. 49-58.

[7] A. Steffens, D. Dinkler and H. Ahrens, "Modeling Carbonation for Corrosion Risk Prediction of Concrete Structures," *Cement and Concrete Research*, Vol. 32, No. 6, 2002, pp. 935-941. doi:10.1016/S0008-8846(02)00728-7

[8] K. K. Adler, "Protection of Concrete against Carbonation," In: R. N. Swamy, Ed., *Proceedings of the International Conference on Corrosion and Corrosion Protection of Steel in Concrete*, Sheffield, 24-28 July 1994, pp. 1081-1093.

[9] Th. Zafeiropoulou, E. Rakanta and G. Batis, "Performance Evaluation of organic Coatings against Corrosion in Reinforced Cement Mortars," *Progress in Organic Coatings* Vol. 72, No. 1-2, 2011, pp. 175-180. doi:10.1016/j.porgcoat.2011.04.005

[10] Th. Zafeiropoulou, E. Rakanta and G. Batis, "Industrial Coatings for High Performance Application: Physicochemical Characteristics and Anti-Corrosive Behavior," Brick and mortar research, Chapter 9, 2012, pp. 245-258.

[11] Th. Zafeiropoulou, E. Rakanta and G. Batis, "Novel Coatings: Physicochemical Characteristics and Corrosion Evaluation," 12*th International Conference on Recent Advances in Concrete Technology and Sustainability Issues*, Prague, 30 October-1 November 2012, 24 Pages.

[12] Hellenic Organization for Standardization ELOT 452, "Determination of Total Hg Content to Water with Atomic Absorption Spectroscopy," Athens, 1983.

[13] Hellenic Organization for Standardization ELOT 1421-3, "Steel for the Reinforcement of Concrete—Weldable Reinforcing Steel—Part 3: Technical Class B500C", Athens, 2005.

[14] ISO/DIS 8407.3, "Procedures for Removal of Corrosion Products from Corrosion Test Specimen," Genève, 1986.

[15] American Society for Testing and Materials D 6132-08, "Standard Test Method for Nondestructive Measurement of Dry Film Thickness of Applied Organic Coatings Using an Ultrasonic Gage," Vol. 6, No. 1, 2008.

[16] American Society for Testing and Materials C876-87, "Standard Test Method for Half-Cell Potentials of Reinforcing Steel in Concrete," Vol. 3, No. 2, 1987.

[17] F. Mansfeld, "An Evaluation of Polarization Resistance Measurements," *Werkstoffe und Korrosion*, Vol. 28, No. 1, 1977, pp. 6-11. doi:10.1002/maco.19770280103

[18] American Society for Testing and Materials G59-97(2009), "Standard Test Method for Conducting Potentiodynamic Polarization Resistance Measurements," Vol. 3, No. 2, 2009.

[19] RILEM CPC-18, "Measurement of Hardened Concrete Carbonation Depth," 1988.

[20] J. Crank, "The Mathematics of Diffusion," Oxford University Press, Oxford, 1975.

[21] M. A. Sanjuαn and C. del Olmo, "Carbonation Resistance of One Industrial Mortar Used as a Concrete Coating," *Building and Environment*, Vol. 36, No. 8, 2001, pp. 949-953. doi:10.1016/S0360-1323(00)00045-7

[22] N. Kouloumbi and G. Batis, "The anticorrosive Effect of Fly Ash, Slag and a Greek Pozzolan in Reinforced Con-crete," *Cement and Concrete Composites*, Vol. 16, No. 4, 1994, pp. 253-260. doi:10.1016/0958-9465(94)90037-X

[23] G. Batis, P. Pantazopoulou and A. Routoulas, "Corrosion Protection Investigation of Reinforcement by Inorganic Coating in the Presence of Alkanolamine-Based Inhibitor," *Cement and Concrete Composites*, Vol. 25, No. 3, 2003, pp. 371-377. doi:10.1016/S0958-9465(02)00061-6

[24] N. Kouloumbi and G. Batis, "The anticorrosive Effect of Fly Ash, Slag and a Greek Pozzolan in Reinforced Con-crete," *Cement and Concrete Composites*, Vol. 16, No. 4, 1994, pp. 253-260. doi:10.1016/0958-9465(94)90037-X